TISSUE ENGINEERING: Part A
Volume 17, Numbers 13 and 14, 2011

DOI: 10.1089/ten.tea.2010.0503

Roles of SATB2 in Osteogenic Differentiation and Bone Regeneration

Jin Zhang, D.D.S., Ph.D.,[1,2] Qisheng Tu, M.D., Ph.D.,[1] Rudolf Grosschedl, Ph.D.,[3] Min Seok Kim, D.M.D.,[1] Terrence Griffin, D.M.D.,[4] Hicham Drissi, Ph.D.,[5] Pishan Yang, D.D.S., Ph.D.,[2] and Jake Chen, D.D.S., Ph.D.[1]

Expressed in branchial arches and osteoblast-lineage cells, special AT-rich sequence-binding protein (SATB2) is responsible for preventing craniofacial abnormalities and defects in osteoblast function. In this study, we transduced SATB2 into murine adult stem cells, and found that SATB2 significantly increased expression levels of bone matrix proteins, osteogenic transcription factors, and a potent angiogenic factor, vascular endothelial growth factor. Using an osterix (Osx) promoter-luciferase construct and calvarial cells isolated from runt-related transcription factor 2 (Runx2)-deficient mice, we found that SATB2 upregulates Osx expression independent of Runx2, but synergistically enhances the regulatory effect of Runx2 on Osx promoter. We then transplanted SATB2-overexpressing adult stem cells genetically double-labeled with bone sialoprotein (BSP) promoter-driven luciferase and β-actin promoter-driven enhanced green fluorescent protein into mandibular bone defects. We identified increased luciferase-positive cells in SATB2-overexpressing groups, indicating more transplanted cells undergoing osteogenic differentiation. New bone formation was consequently accelerated in SATB2 groups. In conclusion, SATB2 acts as a potent transcription factor to enhance osteoblastogenesis and promote bone regeneration. The application of SATB2 in bone tissue engineering gives rise to a higher bone forming capacity as a result of multiple-level amplification of regulatory activity.

Introduction

As a nuclear matrix protein, special AT-rich sequence-binding protein 2 (SATB2) activates gene transcription through binding to nuclear matrix-attachment regions, which are AT-rich DNA sequences implicated in the regulation of gene transcription by altering the organization of eukaryotic chromosomes, structurally defining the borders of chromatin domains, and augmenting the potential of enhancers to act over large distances.[1–3] While binding to AT-rich DNA elements, SATB2 modifies the chromatin structure through interacting with histone deacetylase 1 and metastasis-associated protein 2, and thus plays an important role in integrating genetic and epigenetic signals.[4] The matrix-attachment region-binding ability and transcriptional activation potential of SATB2 can be increased by mutations of two lysines that remove the inhibitory modification by the covalent conjugation of the small ubiquitin-related modifier.[2]

The *SATB2* gene lies in a gene-poor region of 2q32–q33, on which a locus for isolated cleft palate is located.[5] In 2003 *SATB2* was identified as the cleft palate gene on 2q32-q33, and haploinsufficiency of *SATB2* was reported to affect multiple systems in humans.[6] Indeed, an individual with a *de novo* germline nonsense in *SATB2* was reported to exhibit generalized osteoporosis, profound mental retardation, and craniofacial dysmorphism, including cleft palate, mandibular hypoplasia, and protruding incisors.[7] In another four patients with an interstitial deletion of chromosome 2q32–q33, similar clinical findings were reported including growth retardation, distinct facial dysmorphism, and a cleft or high palate which was considered to be the result of hemizygosity for *SATB2*.[8] Based on the common clinical features in individuals with small deletions of 2q32-q33, researchers suggested that microdeletions of 2q32-q33 constitute a distinct syndrome characterized with palate abnormalities, tooth anomalies, growth retardation, and behavior problems (OMIM 612313), and *SATB2* haploinsufficiency is the etiological factor for, at least, some of the clinical features associated with this syndrome.[8,9]

SATB2 and murine *Satb2* are highly conserved (99.6%), and animal studies have recently confirmed an essential role of SATB2 in proper facial patterning of the embryo and in

[1]Division of Oral Biology, Department of General Dentistry, Tufts University School of Dental Medicine, Boston, Massachusetts.
[2]School of Stomatology, Shandong University, Jinan, Shandong Province, China.
[3]Department of Cellular and Molecular Immunology, Max-Planck Institute of Immunobiology, Freiburg, Germany.
[4]Department of Periodontics, Tufts University School of Dental Medicine, Boston, Massachusetts.
[5]Department of Orthopaedic Surgery, University of Connecticut, Farmington, Connecticut.

normal bone development.[9] *Satb2*$^{-/-}$ embryos showed multiple craniofacial defects, including a significant truncation of the mandible and a cleft palate,[10,11] which resemble the clinical manifestations observed in humans with genetic aberrations in the *SATB2* gene.[11] *Satb2*$^{-/-}$ mice also exhibited defects in osteoblast differentiation and function, which consequently delayed bone formation and mineralization.[10] The defects observed in *Satb2*-null mice have been attributed to an increased expression of specific members of the Hox gene clusters and a decreased expression of osteoblast-specific genes, whereby SATB2 was shown to regulate these genes at the chromatin level.[10]

Vertebrate skeletogenesis involves two processes, skeletal patterning and osteoblast differentiation. Previous studies clearly demonstrated that SATB2 plays pivotal roles in both processes, suggesting that SATB2 can be used as an ideal bioactive factor to overcome the hurdles in craniofacial and dental regeneration by providing functional bone tissue with natural morphology and physiological properties. In this study, we further investigated the role of SATB2 in osteogenic differentiation, and made the first step to the application of this novel transcription factor in tissue engineering to promote bone regeneration.

Materials and Methods

Plasmids

The mouse *Satb2* cDNA was released from pBs-SK-*Satb2* (from Dr. Rudolf Grosschedl, Max-Planck Institute of Immunobiology, Freiburg, Germany),[10] and was ligated into pBABE-hygro (Addgene ID: 1765) and pcDNA3.1(+) (Invitrogen). A 4.1-kb DNA fragment was released from pBs-SK-*Satb2* by double digestion with *Not*I/*Eco*RV, blunted, and self-ligated, resulting in a plasmid with a 1000 bp fragment of *Satb2* cDNA. The 1000 bp fragment of *Satb2* cDNA was then released and ligated into the plasmid pBluescript-SKII (+), creating pBs-SKII-*Satb2* (1000 bp) to be used to prepare a 1000 bp *Satb2* probe for *in situ* hybridization. pcDNA3.1-*Bmp4* was created by subcloning mouse *Bmp4* polymerase chain reaction (PCR) fragments into pcDNA3.1(+) (Invitrogen). The full-length osterix (Osx) promoter-luciferase construct (−2020/+13) was produced in Dr. Hicham Drissi's laboratory at University of Connecticut Health Center, Farmington, CT.[12] A plasmid encoding *Runx2* (pCMV-*Osf2*/*Cbfa1*) was a gift from Dr. Karsenty's laboratory (College of Physicians and Surgeons, Columbia University, New York, NY).

In situ *hybridization*

In situ hybridization for the detection of *in vivo* distribution of the *Satb2* mRNA was performed essentially as described previously.[13] Briefly, E14.5 embryos were isolated from C57BL/6J mice, fixed in 4% paraformaldehyde, and embedded in paraffin. Tissue sections, 6 μm in thickness, were mounted on glass slides for *in situ* hybridization studies. The 1000 bp *Satb2* cDNA fragment was released from pBs-SKII-*Satb2* (1000 bp) and *in vitro* transcribed using a MAXIscript *In Vitro* Transcription Kit (Ambion) and 5′-[^{35}S]UTP (1250 Ci/mmol). The tissue sections were then deparaffinized and incubated with ^{35}S-labeled RNA probe. Control sections were incubated with sense cRNA probes under the same conditions. The tissue sections were then dipped in Kodak NTB-2 emulsion (Eastman Kodak Company), and developed after 3 days of exposure. Tissue sections were counterstained with hematoxylin and eosin (H&E), and observed using a Nikon Eclipse E600 microscope.

Cell culture

MC3T3-E1 murine osteoblast-like cells were maintained in alpha minimum essential medium (α-MEM) with 10% fetal bovine serum and antibiotics. Murine osteoblast precursor cells in the form of calvarial cells were isolated and routinely cultured as described previously.[14] Dental follicle cells (DFCs) and bone marrow stromal cells (BMSCs) were obtained from 5–7-day-old or 7-week-old BSP-Luc/ACTB-EGFP mice, respectively, and were cultured as described previously.[15,16] Briefly, for DFCs, bilateral first mandibular molar germs were dissected and digested with 1% trypsin at 4°C for 1.5 h. The dental follicle tissues were then isolated and cultured in α-MEM supplemented with 20% fetal bovine serum and antibiotics. Bone siloprotein-Luc/ACTB-EGFP mice were genetically double labeled with a luciferase reporter gene driven by a bone sialoprotein (BSP) promoter and an enhanced green fluorescent protein (EGFP) driven by a beta-actin promoter.[15]

Preparation of retroviral vectors and cell infection

pBABE-hygro-*Satb2* and packaging vector pCL-Eco were co-transfected into HEK-293T cells using Lipofectamine Reagent (Invitrogen). Forty-eight hours after transfection, the supernatant filtered through a 0.45 μm filter (Millipore) was used to infect the cells with polybrene at a final concentration of 8 μg/mL. The empty retroviral vector pBABE-hygro was also packaged and used as a control. Stably infected cells were selected using hygromycin B (Invitrogen).

Transient cell transfection and luciferase assay

For transient transfection, the full-length Osx promoter-luciferase construct (−2020/+13) and a β-gal control plasmid were co-transfected with pcDNA3.1-*Satb2*, or pCMV-*Osf2*/*Cbfa1*, or both into HEK-293 and MC3T3-E1 cells using lipofectamine Reagent (Invitrogen). Forty-eight hours after transfection, luciferase and β-gal levels were determined using a luminometer (Lumat LB 9501; EG&G Berthold) and β-gal detection kit II (BD Clontech), respectively. Luciferase activity was normalized to β-galactosidase activity.

Real-time reverse transcription–PCR for mRNA analysis

Quantitative real-time reverse transcription–PCR assay for mRNA analysis was performed using iQ™ SYBR Green Supermix (Bio-Rad Laboratories) on a Bio-Rad iQ5 thermal cycler (Bio-Rad Laboratories). The evaluation of relative differences in PCR product amounts was carried out by the comparative cycle threshold method, using glyceraldehyde 3-phosphate dehydrogenase as a control.

RNA interference and Western blot

Calvarial osteoblasts were transfected with *SATB2* siRNAs or scrambled control siRNAs (Santa Cruz Biotechnology)

following the recommendations of the manufacturer. Whole protein lysates were prepared essentially as described previously.[17] Antibodies for SATB2 (Abcam) and β-actin (Santa Cruz Biotechnology) were used in the Western blot analysis. The secondary antibodies were horseradish peroxidase-linked goat-anti rabbit IgG (Santa Cruz). Blots were observed using electrogenerated chemiluminescence (ECL) reagents from Pierce Biotechnology.

Animal surgery

Collagen matrices purchased from Collagen Matrix, Inc., were trimmed into appropriate size (2.5×2×1 mm), and static seeding techniques were used to transfer SATB2-overexpressing DFCs or BMSCs into the matrix. Briefly, cell suspension at the concentration of 10^6 cells/mL was applied to the respective sponges, which were incubated for 1 h at 37°C and then transplanted to the bone defect sites. Mandibular bone defects were created in 5-month-old B6D2F1 male mice (Jackson Laboratory), the strain from which our mBSP9.0Luc transgenic mice were derived.[13] Bone defects, 1.5 mm in diameter, were created on the bone overlying the mandibular first molar. The generated bone defects were then transplanted with collagen matrix seeded with SATB2-overexpressing BMSCs or DFCs, or corresponding control cells. Animals were sacrificed 7 days after surgery.

Mice were maintained and used in accordance with recommendations in *The Guide for the Care and Use of Laboratory Animals* prepared by the Institute on Laboratory Animal Resources, National Research Council (DHHS Publ. NIH 86–23, 1985), and by guidelines established by the Institutional Animal Care and Use Committee of the Tufts-New England Medical Center (Boston, MA).

Histomorphometric analysis

The isolated bone samples were fixed in 10% neutral-buffered formalin solution, decalcified using 0.2 N HCL, and embedded in paraffin. Tissue sections, 6 μm in thickness, were mounted on glass slides and H&E staining was performed. Digital images were taken with a Nikon Eclipse E600 microscope and analyzed by Spot Advanced software (Diagnostic Instruments). Newly formed bone areas, expressed as a percentage (area of newly formed bone/area of original wound×100), were measured essentially as described previously.[18]

Immunohistochemical staining

Immunohistochemical staining (IHC) was performed using a Histostaining Kit from Zymed Laboratories, Inc. The IHC procedures were described in our previous publications.[13] Control sections were incubated with an irrelevant antibody (anti-human CD4 lymphocyte antigen) to estimate back-ground staining. Primary antibodies against SATB2 (Abcam), firefly luciferase (Santa Cruz Biotechnology), GFP (Clontech), and BSP (a gift from Dr. Larry Fisher, NIH/NIDCR) were purchased. For SATB2 IHC staining, the Histostain-SP Kit (DAB, Broad Spectrum; Invitrogen) was used. For IHC staining of luciferase, GFP, and BSP, the Histostain-SP Kit (AEC, Broad Spectrum; Invitrogen) was used. Stained slides were observed under a Nikon Eclipse E600 microscope and cell counts were performed within the newly formed bone area. The numbers of BSP, GFP, and luciferase-positive cells were normalized to the total number of cells in the wound sites.[15]

Statistical analysis

All results were expressed as means ± standard error of the mean of three or more independent experiments. One-way analysis of variance was used to test significance using the software package Origin 6.1 (OriginLab). Values of $p < 0.05$ were considered statistically significant.

Results

Expression pattern of SATB2 in mouse embryos and adult bone tissues

To get first-hand information of SATB2 expression pattern in the jaws and teeth, we performed *in situ* hybridization of the head from wild-type mice (C57BL/6J) at E14.5. We found that *Satb2* mRNA was highly expressed in the dental mesenchymal components of incisor tooth germ (Fig. 1A, B). Moreover, the signal of *Satb2* mRNA was intense in the developing palate and mandibular bone matrix, but was weak in Meckel's cartilage. The strongest expression of *Satb2* mRNA was observed in the edges of the developing palatine processes, which were growing toward each other (Fig. 1C–F). The expression pattern of *Satb2* mRNA in jaws and teeth indicated that SATB2 plays an important role in the development of these organs. We also performed IHC staining to monitor the expression of SATB2 in E14.5 mouse embryos at the protein level. We observed intense SATB2 signals in the nucleui of osteoblasts aligning on the surface of the developing mandibular bone in the E14.5 mouse embryos (Fig. 2A–D). We also found abundant SATB2-positive cells in the mesenchymal component of the incisor tooth germs (Fig. 2E) and the developing palate (Fig. 2F, G) at this developmental stage. Interestingly, we also found a few SATB2-positive chondrocytes in the Meckel's cartilage, which were seemed to be at their hypertrophic stage (Fig. 2B, D).

SATB2 has been reported to be expressed in the breast tissues and leukocytes in adult human beings.[7,19] In animal models, SATB2 was found to be expressed in adult central nervous system.[20,21] However, currently it is still unclear whether SATB2 is also expressed in adult bone tissues. In this study, we performed IHC staining on femoral bone tissue sections derived from 2-month-old wild-type mice. On these tissue sections, we detected strong signals of SATB2 in the osteoprogenitor cells aligning on the inner surface of the adult femurs (Fig. 2H, I) and the surface of the trabecular bone at the growth plate area (Fig. 2J, K). We also created 1.5 mm bone defects on the mandibles of 5-month-old B6D2F1 mice and monitored the expression of SATB2 protein in the mandibular bone defects. As shown in Figure 2L and M, the collected mandibular bones were cut in the horizontal direction, and we observed intense SATB2 staining in most of the osteoblasts existing in the newly formed bone area of the mandibular bone defects.

SATB2 enhances expressions of bone matrix proteins and osteogenic transcription factors in BMSCs and DFCs

BMSCs and DFCs were known to be able to differentiate into hard tissue forming cells (osteoblasts or cementoblasts),

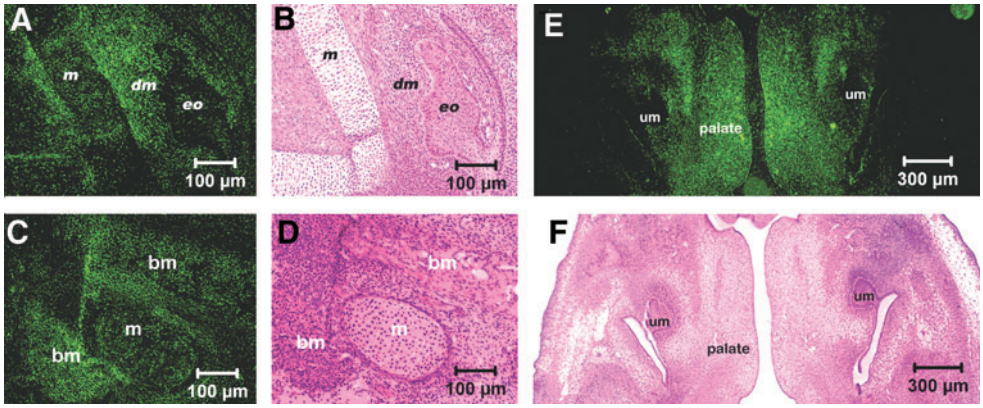

FIG. 1. *In situ* hybridization **(A, C, E)** and H&E staining **(B, D, F)** of the heads from wild-type mice (C57bl/6j) at E14.5. **(A, B)** The *SATB2* gene is strongly expressed in mesenchymal components of incisors. **(C, D)** SATB2 expression is high in bone matrix of mandible, but is weak in the Meckel's cartilage. **(E, F)** SATB2 expression in the edges of developing palatine processes is prominent. m, meckel's cartilage; dm, dental mesenchyme; eo, enamel organ; bm, bone matrix; um, upper molar. H&E, hematoxylin and eosin; SATB2, special AT-rich sequence-binding protein. Color images available online at www.liebertonline.com/tea

and bone marrow mononuclear cells were recently found to promote tissue regeneration in critical size rat cranial defects without the need for *in vitro* culture, expansion, and purification.[22] To investigate the effect of SATB2 on the differentiation processes of BMSCs and DFCs, we transiently transfected pcDNA3.1-*Satb2* into BMSCs and DFCs, and determined gene expression changes. Considering the potent osteogenic inductivity of bone morphogenetic proteins (BMPs), pcDNA3.1-*Bmp4* was also transfected into BMSCs to serve as a positive control. Cells transfected with the empty vector (pcDNA3.1) served as negative controls. We found that 72 h after transfection, SATB2-overexpressing BMSCs showed increased mRNA levels of BSP, runt-related transcription factor 2 (Runx2), Osx, and vascular endothelial growth factor A (VEGFA) compared with the control cells. BMP4 induced the expression of SATB2 at the mRNA level,

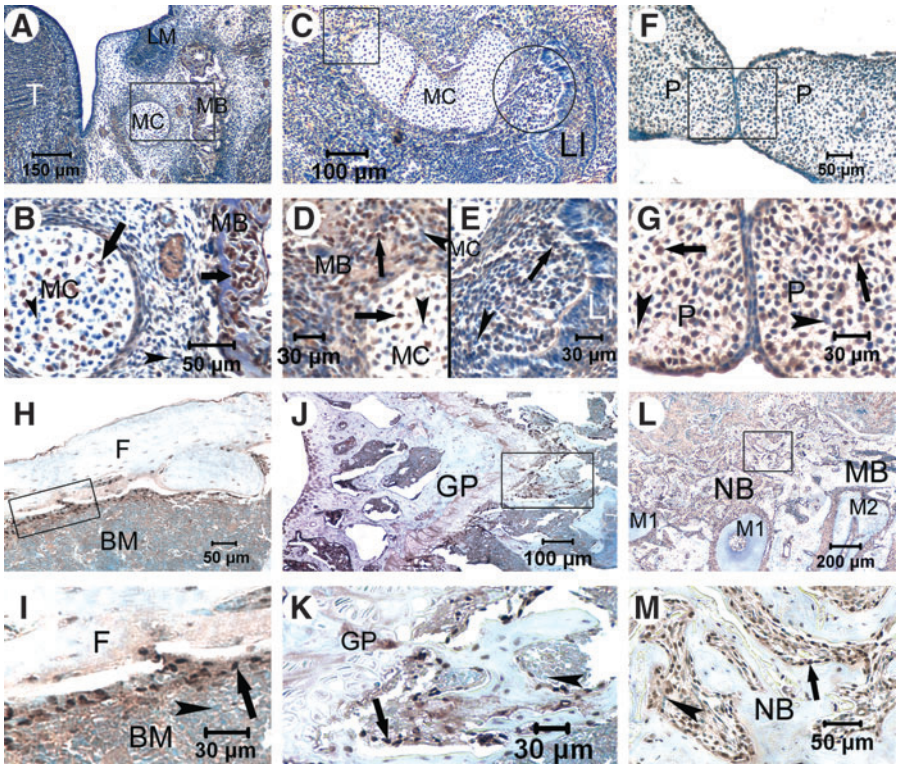

FIG. 2. Immunohistochemical staining of the heads from C57bl/6j mice at E14.5 **(A–G)**, the femurs from 2-month-old C57bl/6j mice **(H–K)**, and the mandubular bone defects created in the 5-month-old B6D2F1 mice **(L, M)**. **(A, B)** Intense SATB2 signals are detected in the nucleui of osteoblasts aligning on the surface of the developing mandibular bone in the E14.5 mouse embryos. Some of the chondrocytes in the Meckel's cartilage are also positively stained. **(B)** Higher magnification of the squared area in **A**. **(C–E)** In addition to the strong staining in the mandibular osteoblasts, abundant SATB2-positive cells are observed in the mesenchymal component of the lower incisor tooth germs. **(D)** Higher magnification of the squared area in **C**. **(E)** Higher magnification of the circled area in **C**. **(F, G)** The developing palate is filled with SATB2-positive cells. **(G)** Higher magnification of the squared area in **F**. **(H, I)** Strong signals of SATB2 are observed in the nuclei of osteoprogenitor cells aligning on the inner surface of the adult femurs. **(I)** Higher magnification of the squared area in **H**. **(J, K)** At the growth plate area of the adult femurs, many SATB2-positive cells attach to the surface of the trabecular bone. **(K)** Higher magnification of the squared area in **J**. **(L, M)** Most of the osteoblasts existing in the newly formed bone area of the mandibular bone defects are strongly stained. The mandibular bones were cut in the horizontal direction. **(M)** Higher magnification of the squared area in **L**. T, tongue; LM, lower molar; MB, mandibular bone; MC, Meckel's cartilage; LI, lower incisor; P, palate; F, femur; BM, bone marrow; GP, growth plate; NB, newly formed bone; M1, roots of the first mandibular molar; M2, roots of the second mandibular molar; arrow, positively stained cells; arrow head, negatively stained cells. Color images available online at www.liebertonline.com/tea

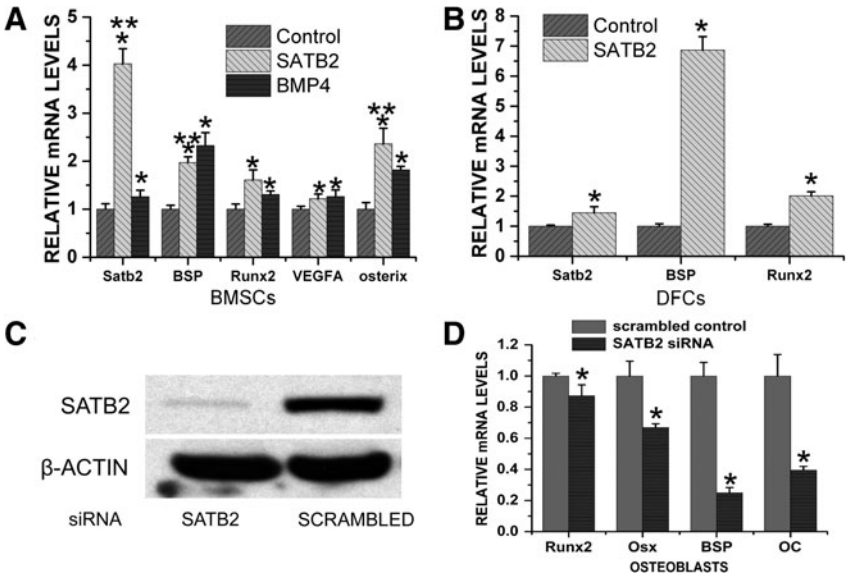

FIG. 3. SATB2 upregulated expression levels of bone matrix proteins and osteogenic transcription factors. **(A)** BMSCs were transiently transfected with pcDNA3.1-*Satb2* or pcDNA3.1-*Bmp4*. BMSCs transiently transfected with pcDNA3.1 served as the negative control. SATB2 overexpression in BMSCs enhanced the mRNA levels of BSP, Runx2, Osx, and vascular endothelial growth factor A. BMP4 increased the mRNA level of SATB2. Data were represented as mean ± SEM. $*p < 0.05$, versus control group (pcDNA3.1 group); $**p < 0.05$, SATB2 group versus BMP4 group. **(B)** DFCs were transiently transfected with pcDNA3.1-*Satb2*. DFCs transiently transfected with pcDNA3.1 served as the negative control. SATB2 overexpression in DFCs also enhanced the mRNA levels of BSP and Runx2. Data were represented as mean ± SEM. $*p < 0.05$, SATB2 group versus control group (pcDNA3.1 group). **(C)** Calvarial osteoblasts were transfected with *SATB2* siRNAs or scrambled control siRNAs (Santa Cruz Biotechnology). SATB2 protein level in these calvarial osteoblasts was dramatically knocked down by the siRNAs specifically targeting *SATB2*. **(D)** Calvarial osteoblasts transfected with *SATB2* siRNAs or scrambled control siRNAs were also subjected to real-time reverse transcription–polymerase chain reaction analysis. Cells transfected with *SATB2* siRNAs displayed decreased mRNA levels of Runx2, Osx, BSP, and OC compared with the cells transfected with scrambled control siRNAs. Data were represented as mean ± SEM. $*p < 0.05$, versus scrambled control group. BMSC, bone marrow stromal cell; SEM, standard error of the mean; DFC, dental follicle cells; BMP 4, bone morphogenetic protein 4; Osx, osterix; Runx2, runt-related transcription factor 2; BSP, bone sialoprotein; OC, osteocalcin.

but the mRNA levels of BSP, Runx2, Osx, and VEGFA induced by BMP4 showed a different pattern compared with those induced by SATB2 (Fig. 3A). We also found that SATB2 overexpression in DFCs significantly enhanced the mRNA levels of BSP and Runx2 (Fig. 3B). Using real-time reverse transcription–PCR analysis, S*atb2* mRNA could be detected in primary DFCs isolated from molars at the root forming stage (data not shown), although it was demonstrated that SATB2 was not expressed in early developmental stages of molar tooth germs.[10] As shown in Figure 3B, S*atb2* mRNA was also detected in DFCs isolated from molars at the root forming stage that were transfected with the empty vector (pcDNA3.1). We then specifically knocked down SATB2 protein level in calvarial osteoblasts using siRNAs specifically targeting *SATB2*. We found that a lower protein level of SATB2 resulted in decreased mRNA levels of Runx2, Osx, BSP, and osteocalcin (Fig. 3C, D).

SATB2 and Runx2 synergistically upregulate Osx expression

To test whether SATB2 upregulates Osx expression level in a Runx2-dependent way, calvarial cells were harvested from $Runx2^{+/-}$ and $Runx2^{-/-}$ mouse fetuses and cultured in a non-osteoinducive medium. Overexpression of SATB2 was achieved through infection with pBABE-hygro-*Satb2*. Cells infected with pBABE-hygro served as control. As shown in Figure 4A and B, SATB2 overexpression resulted in elevated Osx mRNA levels in both $Runx2^{+/-}$ and $Runx2^{-/-}$ calvarial cells compared with their corresponding control cells. We then co-transfected the full-length Osx promoter-luciferase construct (−2020/+13) with pcDNA3.1-*Satb2*, or pCMV-*Osf2/Cbfa1*, or both into HEK-293 and MC3T3-E1 cells. As a result of elevated SATB2 level, the activity of the Osx promoter was enhanced by approximately 1.8- and 1.6-fold, respectively, in MC3T3-E1 and HEK-293 cells. Runx2 overexpression upregulated the activity of the Osx promoter by 2.52 and 1.8-fold, respectively, in MC3T3-E1 and HEK-293 cell lines. The most prominent increase in Osx promoter activity was observed in cells co-transfected with both pcDNA3.1-*Satb2* and pCMV-*Osf2/Cbfa1*, suggesting that SATB2 and Runx2 act synergistically in regulating the expression level of Osx (Fig. 4C).

SATB2 overexpression in adult stem cells promotes osteogenic differentiation and bone tissue regeneration

DFCs and BMSCs used in this study were obtained from BSP-Luc/ACTB-EGFP mice.[15] SATB2 overexpression in BMSCs and DFCs were achieved through infection with pBABE-hygro-*Satb2*. Cells infected with pBABE-hygro served as controls. Infected cells were transplanted into the mandibular wound sites created in 5-month-old B6D2F1 mice, the strain from which our mBSP9.0Luc transgenic mice were derived. The surgical procedures were illustrated in Figure 5A and B, and in Figure 5C we showed an isolated mandibular bone with the 1.5 mm bone defect. As shown in Figure 5D, the mandibular bone samples were dissected, embedded in paraffin, and microtoned in the coronal direction. The 6-μm-thick tissue sections were numbered, and the tissue sections positioned in lines a, b, and c from each animal were collected for further quantitative analysis (Fig. 5D, E). As shown in Figure 6, the newly formed bone area was evaluated on tissue sections using a double-blinded method to prevent observer's bias. For better comparison, we only

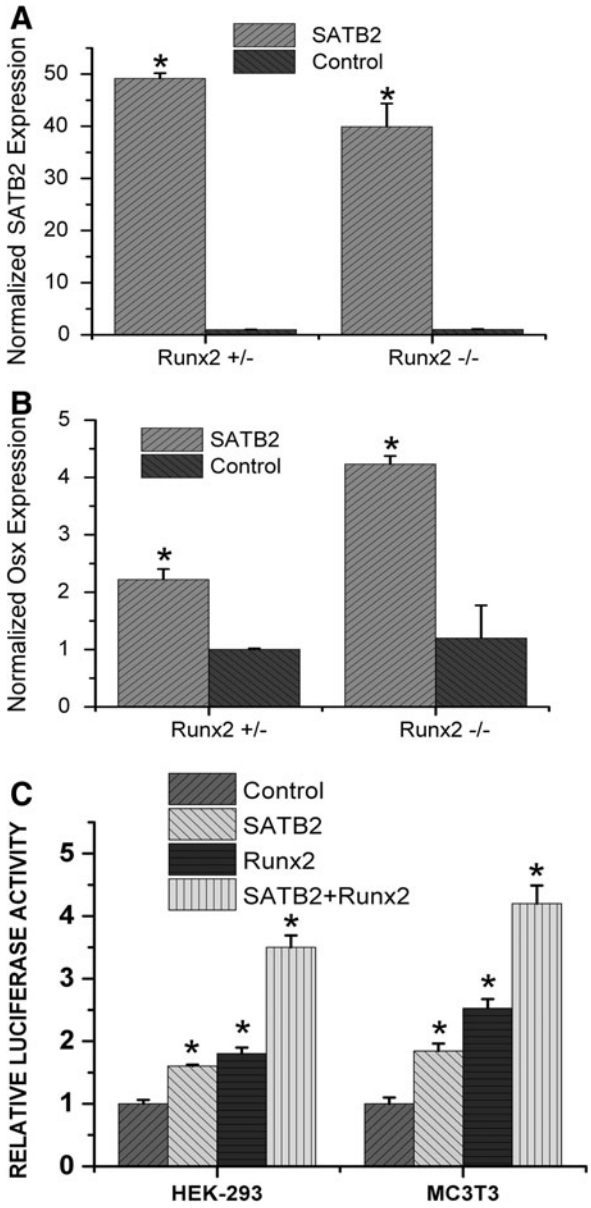

FIG. 4. Effects of SATB2 and Runx2 on the expression level of Osx. **(A, B)** Murine osteoblast precursor cells in the form of calvarial cells were isolated from Runx2$^{+/-}$ and Runx2$^{-/-}$ mice and infected with pBABE-hygro-*Satb2* (SATB2) or pBABE-hygro (control). Expression levels of SATB2 **(A)** and Osx **(B)** were monitored using real-time reverse transcription–polymerase chain reaction analysis. Data were represented as mean ± SEM. *$p < 0.05$, SATB2 group versus control group. **(C)** HEK-293 cells or MC3T3-E1 cells were co-transfected with pOsx2.0kb-luc and a CMV β-gal construct. Empty vector (control), or pcDNA3.1-*Satb2* (SATB2), or pCMV-*Osf2/Cbfa1* (Runx2), or both pcDNA3.1-*Satb2* (SATB2) and pCMV-*Osf2/Cbfa1* (SATB2 + Runx2) were also co-transfected. Luciferase assays were performed to evaluate the effect of SATB2 and Runx2 on Osx promoter activity. Data were represented as mean ± SEM. *$p < 0.05$, versus control group.

illustrated tissue sections collected from position c in the Figure 6. The area within the original bone lesion was assessed by digitizing the reversal line in the bone at the cut margin of the original wound outline. We then digitized the newly formed bone area in the bone compartment of the wound. All of the histomorphometric analysis was performed using Spot Advanced software (Diagnostic Instruments), and the newly formed bone area was expressed as a percentage (area of newly formed bone/area of original wound × 100).

Observation on H&E-stained sections revealed increased newly formed bone tissues in bone defects treated with SATB2-transduced BMSCs (SATB2-BMSC group, Fig. 6B) and DFCs (SATB2-DFC group, Fig. 6E), compared with the corresponding control groups, control-BMSC group (Fig. 6A), and control-DFC group (Fig. 6D), respectively. Histomorphometric analysis confirmed increased newly formed bone area in the two SATB2 groups, indicating that bone tissue regeneration was accelerated by SATB2 overexpression (Fig. 6C, F).

IHC staining was then performed in SATB2-BMSC group and control-BMSC group to track and evaluate the osteogenic ability of the transplanted adult stem cells. As mentioned above, the adult stem cells used in our *in vivo* experiment were isolated from a double-labeled transgenic mouse line, BSP-Luc/ACTB-EGFP mice.[15] Briefly, mBSP9.0Luc mice contain a BSP promoter linked to the luciferase reporter gene (mBSP9.0Luc).[13] A second marker, GFP, was introduced into the mBSP9.0Luc mice by cross breeding these mice with BACT-EGFP mice in which an EGFP is driven by a beta-actin promoter and cytomegalovirus enhancer (#3291, Jackson Lab). The resulted transgenic mice were named as BSP-Luc/ACTB-EGFP mice. All adult stem cells isolated from the BSP-Luc/ACTB-EGFP mice express GFP, and the expression of luciferase is switched on as the cells differentiate into osteoblasts. Therefore, in our study, after the adult stem cells isolated from the BSP-Luc/ACTB-EGFP mice were transplanted into the recipient mice, GFP staining can be used to track the fate and migration of these adult stem cells, whereas Luciferse staining serves as a marker for osteogenic differentiation of the transplanted cells. Using IHC staining, the localization of BSP, luciferase, or GFP was studied on tissue sections collected at the positions of lines a, b, and c as indicated in Figure 5D. At least three tissue sections from each position and altogether at least nine sections from each animal were used for cell counting. Cell counts were performed within the newly formed bone area, and a positively stained cell was defined as a purple-stained nucleus surrounded by red staining. The final data were represented by the ratio of the positively stained cells versus total cells.

In both groups, positive EGFP and luciferase signals could be detected, indicating transplanted exogenous BMSCs and transplanted BMSCs undergoing osteogenic differentiation, respectively (Fig. 7A). Positive cell counting showed a higher number of luciferase-positive cells in SATB2-BMSC group than in control-BMSC group, indicating that SATB2 overexpression significantly enhanced the osteogenic differentiation of transplanted BMSCs (Fig. 7B). Consistent with this result, more BSP-positive cells were observed in SATB2-BMSC group than in the control-BMSC group (Fig. 7C). No statistically significant difference in the number of EFGP-positive cells was detected between SATB2-BMSC group and control-BMSC group (Fig. 7D).

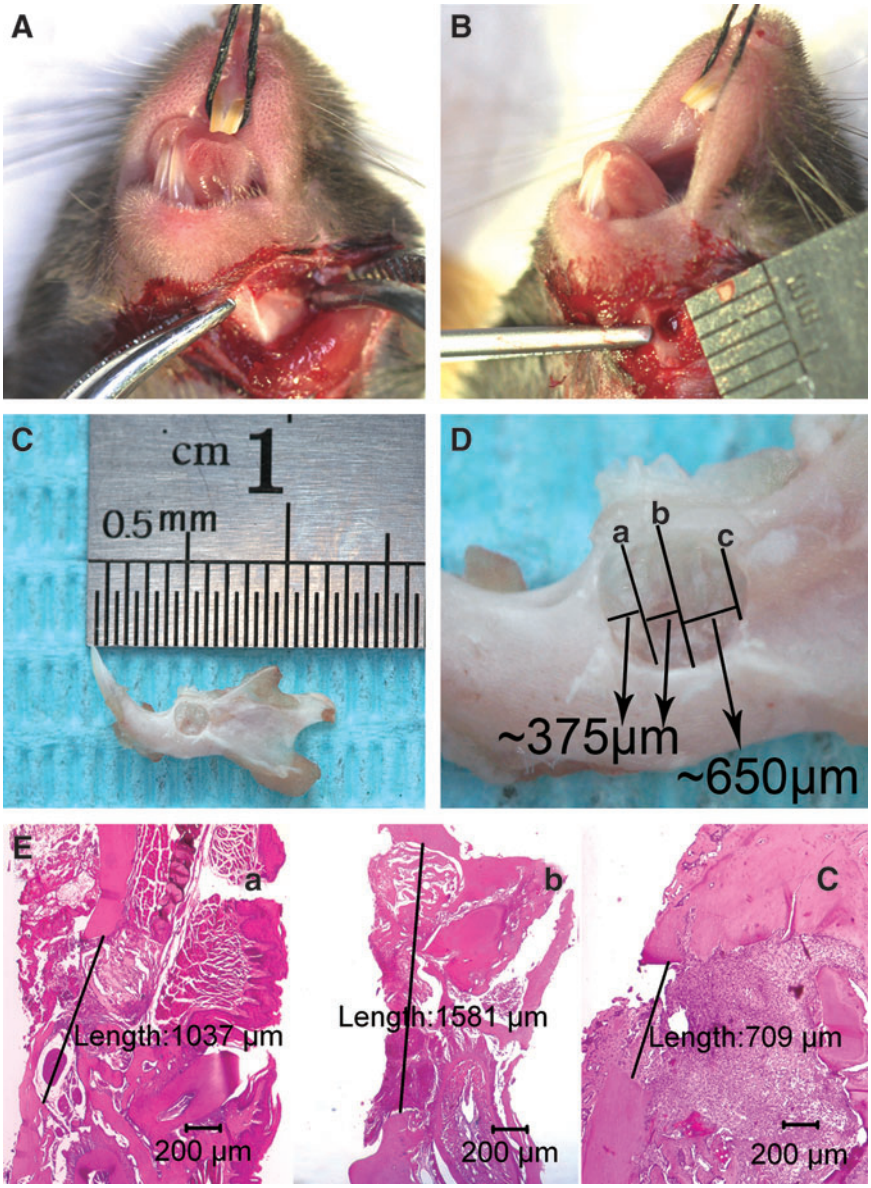

FIG. 5. Surgical procedures and the protocol for histomorphometric analysis. **(A)** Under general anesthesia, a submandibular incision was made, and the masseter was lifted from its insertion in the inferior mandibular border to amply expose the mandible. **(B)** A bone defect, 1.5 mm in diameter, was created on the bone overlying the mandibular first molar with a dental bur (#329, Midwest, 0.6 mm in diameter). **(C)** An isolated mandibular bone with the 1.5 mm bone defect. **(D)** The mandibular bone samples were cut in the coronal direction. The 6-μm-thick tissue sections were numbered, and the tissue sections positioned in lines a, b, and c from each animal were collected for further quantitative analysis. **(E)** Representative photos indicating tissue sections collected at positions a, b, and c, respectively. Color images available online at www.liebertonline.com/tea

Discussion

In our previous studies, we have applied osteogenic molecules in bone tissue engineering to promote osteogenic differentiation and bone regeneration.[18,23] Using a mouse periodontal window wound model, we found that as a result of Runx2 overexpression, local stem cells were induced to differentiate toward osteoblast-lineage cells and participated in the regenerative processes more actively, which significantly enhanced new bone formation.[18] However, while a substantial amount of new bone was formed under the stimulation of Runx2, the engineered alveolar bone was relatively loosening and more cancellous, suggesting that the effect of Runx2 in directing the regenerative tissues toward normal morphological and functional status was still not satisfied for clinical application. Likewise, Osx has proved to play an important role in bone tissue regeneration. It enhances proliferation and osteogenic potential of BMSCs *in vitro*, and stimulates cascade of bone anabolic activity by stimulating healing of critical-sized defects in murine calvarial bone.[23,24] However, the regenerated calvarial bone in Osx treated group was generally thinner and more delicate than the native calvaria. In histological observation, accessory structures such as bone sutures were not formed, suggesting that possible factors that regulate embryonic bone development are missing in the adult bone regeneration process. We speculate that there might be other factors involved in the morphogenesis and remodeling in bone regeneration.

As a transcription regulator, SATB2 functions broadly and plays an important role in craniofacial patterning and bone development, making it a plausible candidate gene for bone tissue engineering. SATB2 not only enhances osteogenic differentiation through positively regulating expression of multiple osteoblast-specific genes, but also promotes bone formation and participates in branchial arch patterning through repressing several Hox, genes including *Hoxa2*.[10] Acting as a "molecular node" in a transcriptional network

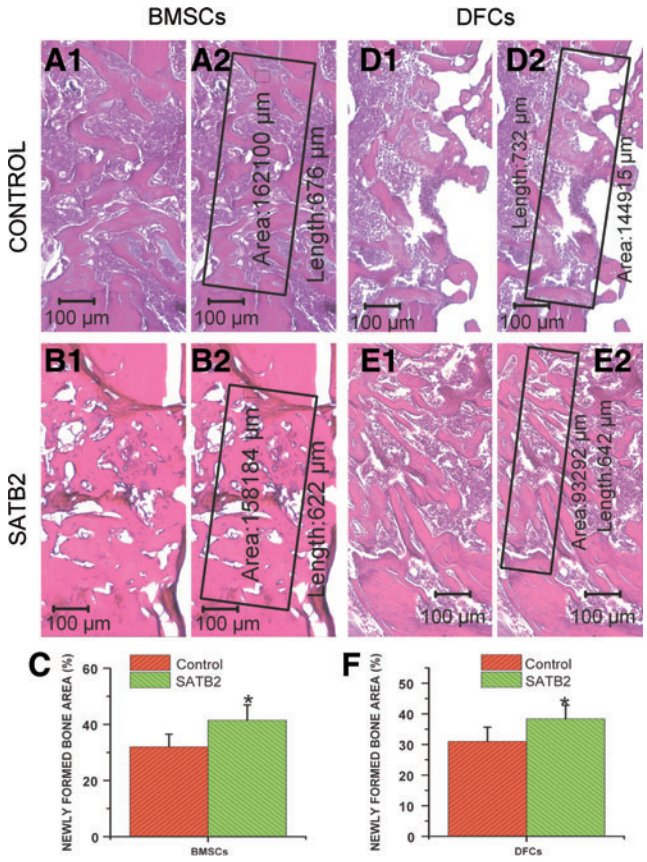

FIG. 6. Histological analysis demonstrated increased bone tissue regeneration and mineralization in bone defects exposed to SATB2-overexpressing adult stem cells. **(A, B)** H&E-stained sections showing bone defects transplanted with control BMSCs **(A)** or SATB2-overexpressing BMSCs **(B)**. **A2** and **B2** are exactly the same images as **A1** and **B1**, respectively; however, we showed, in **A2** and **B2**, the area within the original bone lesion assessed by digitizing the reversal line in the bone at the cut margin of the original wound outline. **(C)** Histomorphometric analysis showed an elevated newly formed bone area in bone defects treated with SATB2-overexpressing BMSCs. Data were represented as mean ± SEM. $*p < 0.05$, SATB2 group versus control group. **(D, E)** H&E-stained sections showing bone defects transplanted with control DFCs **(D)** or SATB2-overexpressing DFCs **(E)**. Again in **D2** and **E2**, we showed the area within the original bone lesion assessed by digitizing the reversal line in the bone at the cut margin of the original wound outline. **(F)** The newly formed bone area was higher in bone defects treated with SATB2-overexpressing DFCs, as indicated by histomorphometric analysis. Data were represented as mean ± SEM. $*p < 0.05$, SATB2 group versus control group. Color images available online at www.liebertonline.com/tea

regulating bone development and osteoblast differentiation, SATB2 interacts with and enhances the transcriptional activity of Runx2 and ATF4, two transcription factors that play essential roles in inducing osteogenic differentiation.[10] Consistent with these previous findings, we found that SATB2 overexpression significantly enhances expressing levels of bone matrix proteins and osteogenic transcription factors. SATB2 also increases the expression level of VEGF, a major angiogenic factor. Localized and sustained VEGF delivery results in greater bone regeneration in calvarial defects than observed with scaffold implantation alone.[25] Furthermore, the combined delivery of angiogenic and osteogenic factors has been demonstrated to promote bone formation and healing.[26] The upregulation of VGEF by SATB2 strongly indicated a potential role of SATB2 in promoting angiogenesis during tissue regeneration. The expression of SATB2 in DFCs of molar tooth germs during root forming stage indicated that SATB2 may also function in the process of root formation.

Recently, transgenic mice overexpressing Runx2 in osteoblasts under the control of the collagen I promoter have been shown to exhibit severe osteopenia and fragile bones due to inhibition of the late stage of osteoblast maturation.[27] These results suggest that new bone formation might occur more efficiently and lead to bone matrix of better quality *in vivo* if Runx2 levels are high during the early differentiation stage and low during the osteoblast maturation stage. Our previous studies proved that although Osx did not increase Runx2 expression, it did promote bone regeneration, and a high ratio of Osx to Runx2 at the late stages of osteoblast differentiation may be essential for the efficient formation of newly engineered bone.[24] In this study, we found that SATB2 not only upregulates Osx expression independent of Runx2, but also synergistically enhances the increase in Osx expression mediated by Runx2, demonstrated that by regulating the ratio of other important transcription factors, SATB2 may promote osteogenic differentiation and improve the quality of newly formed bone.

Taken together, SATB2 can be a robust osteo-inductive molecule recruiting other transcription factors to form a platform or act as a molecular node for a transcriptional network. It can synergize, amplify, and thus exponentially augment the activity of multiple osteogenic transcriptional factors, including Runx2, Osx, and ATF4, to regulate skeletal development and osteoblast differentiation in craniofacial reconstruction. Craniofacial and dental structures represent the most complex organs in human body, and the application of SATB2 in bone tissue engineering of the craniofacial region may give rise to a higher bone forming capacity as a result of multiple-level amplification of regulatory activity.

To investigate the capacity of SATB2 to promote bone regeneration, we performed *in vivo* studies and transplanted SATB2-transduced BMSCs or DFCs into bone defects created in B6D2F1 mice. The BMSCs and DFCs used in this study were isolated from a unique double-labeled transgenic mouse line designated BSP-Luc/ACTB-EGFP mice.[15] Briefly, the β-actin promoter-driven EGFP enables us to identify every exogenous cell from host cells present in the wound sites, whereas the BSP promoter-driven luciferase is switched on as the transplanted cells differentiate into osteoblasts or cementoblasts. In this way, the *in vivo* role of SATB2 on the survival, migration, and differentiation of the transplanted BMSCs can be conveniently evaluated and confirmed.

Using these double-labeled cells and a mandibular bone defect model, we found that SATB2 significantly enhances regeneration of damaged mandibular bone tissues, as indicated by increased new bone formation in bone defects transplanted with SATB2-transduced adult stem cells. In addition, IHC staining and cell counting results showed increased luciferase-positive cells and BSP-positive cells in bone defects transplanted with SATB2-transduced BMSCs compared with those transplanted with control BMSCs, although the amount of total transplanted cells in

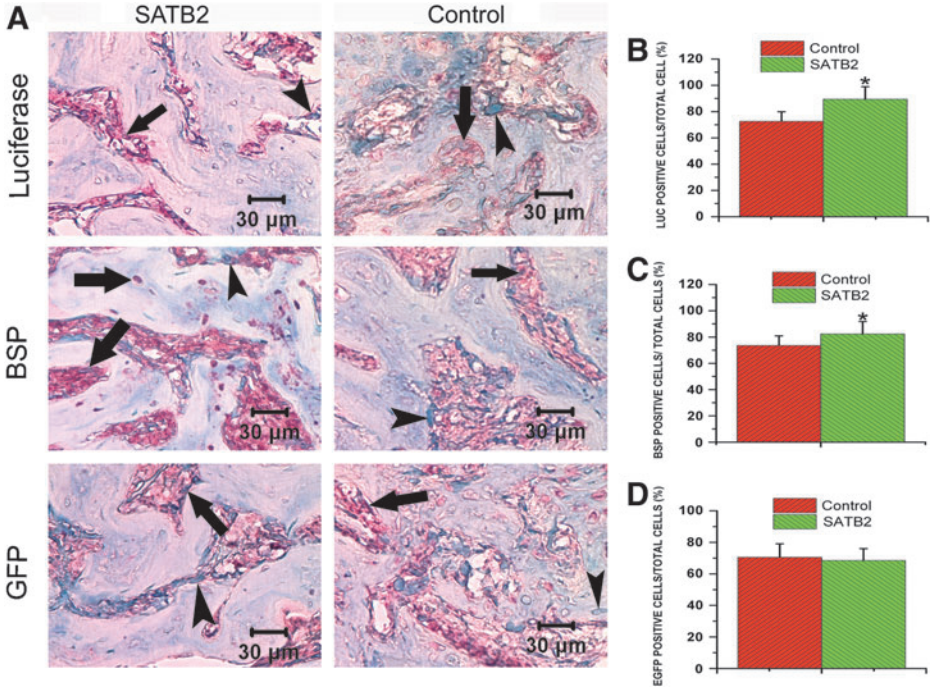

FIG. 7. **(A)** Immunohistochemical staining for Luciferase, BSP, and GFP demonstrated increased Luciferase and BSP expression, which indicated enhanced osteogenic differentiation in SATB2 groups. Cell counting was performed in the whole newly formed bone area as shown in **A2**, **B2**, **D2**, and **E2** of Figure 6. Arrow, positively stained cells; arrow head, negatively stained cells. **(B–D)** Cell counting results indicated that there were more luciferase **(B)** and BSP **(C)** positive cells in SATB2 group than in control group. However, there is no significant difference in GFP-positive cell numbers between these two groups **(D)**. Data were represented as mean ± SEM. $^*p < 0.05$, SATB2 group versus control group. GFP, green fluorescent protein. Color images available online at www.liebertonline.com/tea

SATB2-BMSCs group was similar to that in control-BMSCs group, as represented by the number of EGFP-positive cells. These results, together with our *in vitro* findings, indicated that by orchestrating the expression of a group of osteogenic transcription factors and matrix proteins, SATB2 stimulates more adult stem cells to differentiate toward bone forming cells and regenerate high-quality bone tissues *in vivo*. In oral and maxillofacial surgery practice, a lack of sufficient material precludes the universal use of autogenous bone, whereas the use of allogenic bone for transplantation carries potential risks of immune responses, pathogen transmission, and the necessary immunosuppression. As a promising alternative strategy to accelerate bone regeneration, application of SATB2 in bone tissue engineering provides novel and important insights into gene-therapy and molecular control of orofacial and dental tissue regeneration, which may be applied clinically for tissue engineering in future studies.

In conclusion, SATB2 orchestrates the expression of a group of osteogenic transcription factors and matrix proteins and thus plays a pivotal role in craniofacial development and osteoblastogenesis. For the first time we initiate a new strategy in bone tissue regeneration and reconstruction, showing that SATB2 enhances the osteogenic capacity of adult stem cells to regenerate new bone tissues with high quality. These *in vitro* and *in vivo* findings shed light on the understanding of cell differentiation processes in the complex orofacial structures, and have a great potential in developing new gene-therapy approaches to treat the large population of patients suffering from bone loss diseases.

Acknowledgments

This work was supported by National Institutes of Health grants DE14537 and DE16710 to J.C. We appreciate the technical supports from Jean Tang, Peter Shin, and Erika Brewer.

Disclosure Statement

No competing financial interests exist.

References

1. Scheuermann, R.H., and Garrard, W.T. MARs of antigen receptor and co-receptor genes. Crit Rev Eukaryot Gene Expr **9,** 295, 1999.
2. Dobreva, G., Dambacher, J., and Grosschedl, R. SUMO modification of a novel MAR-binding protein, SATB2, modulates immunoglobulin mu gene expression. Genes Dev **17,** 3048, 2003.
3. Bode, J., Benham, C., Knopp, A., and Mielke, C. Transcriptional augmentation: modulation of gene expression by scaffold/matrix-attached regions (S/MAR elements). Crit Rev Eukaryot Gene Expr **10,** 73, 2000.
4. Gyorgy, A.B., Szemes, M., de Juan Romero, C., Tarabykin, V., and Agoston, D.V. SATB2 interacts with chromatin-remodeling molecules in differentiating cortical neurons. Eur J Neurosci **27,** 865, 2008.
5. Brewer, C.M., Leek, J.P., Green, A.J., Holloway, S., Bonthron, D.T., Markham, A.F., and FitzPatrick, D.R. A locus for isolated cleft palate, located on human chromosome 2q32. Am J Hum Genet **65,** 387, 1999.
6. FitzPatrick, D.R., Carr, I.M., McLaren, L., Leek, J.P., Wightman, P., Williamson, K., Gautier, P., McGill, N., Hayward, C., Firth, H., Markham, A.F., Fantes, J.A., and Bonthron, D.T. Identification of SATB2 as the cleft palate gene on 2q32-q33. Hum Mol Genet **12,** 2491, 2003.
7. Leoyklang, P., Suphapeetiporn, K., Siriwan, P., Desudchit, T., Chaowanapanja, P., Gahl, W.A., and Shotelersuk, V. Heterozygous nonsense mutation SATB2 associated with cleft palate, osteoporosis, and cognitive defects. Hum Mutat **28,** 732, 2007.
8. Van Buggenhout, G., Van Ravenswaaij-Arts, C., Mc Maas, N., Thoelen, R., Vogels, A., Smeets, D., Salden, I., Matthijs, G., Fryns, J.P., and Vermeesch, J.R. The del(2)(q32.2q33)

deletion syndrome defined by clinical and molecular characterization of four patients. Eur J Med Genet **48,** 276, 2005.
9. Rosenfeld, J.A., Ballif, B.C., Lucas, A., Spence, E.J., Powell, C., Aylsworth, A.S., Torchia, B.A., and Shaffer, L.G. Small deletions of SATB2 cause some of the clinical features of the 2q33.1 microdeletion syndrome. PLoS One **4,** e6568, 2009.
10. Dobreva, G., Chahrour, M., Dautzenberg, M., Chirivella, L., Kanzler, B., Farinas, I., Karsenty, G., and Grosschedl, R. SATB2 is a multifunctional determinant of craniofacial patterning and osteoblast differentiation. Cell **125,** 971, 2006.
11. Britanova, O., Depew, M.J., Schwark, M., Thomas, B.L., Miletich, I., Sharpe, P., and Tarabykin, V. Satb2 haploinsufficiency phenocopies 2q32-q33 deletions, whereas loss suggests a fundamental role in the coordination of jaw development. Am J Hum Genet **79,** 668, 2006.
12. Nishio, Y., Dong, Y., Paris, M., O'Keefe, R.J., Schwarz, E.M., and Drissi, H. Runx2-mediated regulation of the zinc finger Osterix/Sp7 gene. Gene **372,** 62, 2006.
13. Paz, J., Wade, K., Kiyoshima, T., Sodek, J., Tang, J., Tu, Q., Yamauchi, M., and Chen, J. Tissue- and bone cell-specific expression of bone sialoprotein is directed by a 9.0 kb promoter in transgenic mice. Matrix Biol **24,** 341, 2005.
14. Tu, Q., Zhang, J., Paz, J., Wade, K., Yang, P., and Chen, J. Haploinsufficiency of Runx2 results in bone formation decrease and different BSP expression pattern changes in two transgenic mouse models. J Cell Physiol **217,** 40, 2008.
15. Li, S., Tu, Q., Zhang, J., Stein, G., Lian, J., Yang, P.S., and Chen, J. Systemically transplanted bone marrow stromal cells contributing to bone tissue regeneration. J Cell Physiol **215,** 204, 2008.
16. Pan, K., Sun, Q., Zhang, J., Ge, S., Li, S., Zhao, Y., and Yang, P. Multilineage differentiation of dental follicle cells and the roles of Runx2 over-expression in enhancing osteoblast/cementoblast-related gene expression in dental follicle cells. Cell Prolif 43, 219, 2010.
17. Valverde, P., Tu, Q., and Chen, J. BSP and RANKL induce osteoclastogenesis and bone resorption synergistically. J Bone Miner Res **20,** 1669, 2005.
18. Tu, Q., Zhang, J., James, L., Dickson, J., Tang, J., Yang, P., and Chen, J. Cbfa1/Runx2-deficiency delays bone wound healing and locally delivered Cbfa1/Runx2 promotes bone repair in animal models. Wound Repair Regen **15,** 404, 2007.
19. Patani, N., Jiang, W., Mansel, R., Newbold, R., and Mokbel, K. The mRNA expression of SATB1 and SATB2 in human breast cancer. Cancer Cell Int **9,** 18, 2009.
20. Maeda, N., Onimura, M., Ohmoto, M., Inui, T., Yamamoto, T., Matsumoto, I., and Abe, K. Spatial differences in molecular characteristics of the pontine parabrachial nucleus. Brain Res **1296,** 24, 2009.
21. Apostolova, G., Loy, B., Dorn, R., and Dechant, G. The sympathetic neurotransmitter switch depends on the nuclear matrix protein Satb2. J Neurosci **30,** 16356, 2010.
22. Kretlow, J.D., Spicer, P.P., Jansen, J., Vacanti, C.A., Kasper, F.K., and Mikos, A.G. Uncultured marrow mononuclear cells delivered within fibrin glue hydrogels to porous scaffolds enhance bone regeneration within critical size rat cranial defects. Tissue Eng Part A, **16,** 3555, 2010.
23. Tu, Q., Valverde, P., Li, S., Zhang, J., Yang, P., and Chen, J. Osterix overexpression in mesenchymal stem cells stimulates healing of critical-sized defects in murine calvarial bone. Tissue Eng **13,** 2431, 2007.
24. Tu, Q., Valverde, P., and Chen, J. Osterix enhances proliferation and osteogenic potential of bone marrow stromal cells. Biochem Biophys Res Commun **341,** 1257, 2006.
25. Banfi, A., Bianchi, G., Notaro, R., Luzzatto, L., Cancedda, R., and Quarto, R. Replicative aging and gene expression in long-term cultures of human bone marrow stromal cells. Tissue Eng 8, 901, 2002.
26. Hsiong, S.X., and Mooney, D.J. Regeneration of vascularized bone. Periodontol 2000 **41,** 109, 2006.
27. Liu, W., Toyosawa, S., Furuichi, T., Kanatani, N., Yoshida, C., Liu, Y., Himeno, M., Narai, S., Yamaguchi, A., and Komori, T. Overexpression of Cbfa1 in osteoblasts inhibits osteoblast maturation and causes osteopenia with multiple fractures. J Cell Biol **155,** 157, 2001.

Address correspondence to:
Jake Chen, D.D.S., Ph.D.
Division of Oral Biology
Department of General Dentistry
Tufts University School of Dental Medicine
One Kneeland St.
Boston, MA 02111

E-mail: jk.chen@tufts.edu

Pishan Yang, D.D.S., Ph.D.
School of Stomatology
Shandong University
44 West Wen Hua Road
Jinan, Shandong Province 250012
P.R. China

E-mail: yangps@sdu.edu.cn

Received: August 26, 2010
Accepted: March 07, 2011
Online Publication Date: April 19, 2011